Nonclassical CD4 + CD49b + Regulatory T Cells as a Better Alternative to Conventional CD4 + CD25 + T Cells To Dampen Arthritis Severity

Rita Vicente, Julie Quentin, Anne-Laure Mausset-Bonnefont, Paul Chuchana, Delphine Martire, Maïlys Cren, Christian Jorgensen, Pascale Louis-Plence

Non-classical CD4$^+$CD49b$^+$ regulatory T cells as a better alternative to conventional CD4$^+$CD25$^+$ T cells to dampen arthritis severity

Rita Vicente[1*,†,‡], Julie Quentin[1*,†,‡], Anne-Laure Mausset-Bonnefont*,†,‡, Paul Chuchana*,†,‡, Delphine Martire*,†,‡, Maïlys Cren†,‡, Christian Jorgensen*,†,‡, and Pascale Louis-Plence*,†,‡

* Inserm, U1183, Institute of Regenerative Medicine and Biotherapies, Montpellier, France

† University of Montpellier, Montpellier, France.

‡ CHU Saint Eloi, Institute of Regenerative Medicine and Biotherapies, Montpellier, France

[1] equally contributed to the study

Address correspondence to: Dr. Pascale Louis-Plence, Inserm U1183, IRMB, 80 rue Augustin Fliche, 34295 Montpellier cedex 05, France.

Phone: (+33) 467 33 57 21/ Fax: (+33) 467 33 01 13

Email: pascale.plence@inserm.fr

Running title: CD49b$^+$ Treg cells express multiple canonical Treg markers

Footnote:

This work was supported in part by research funding from the European Union project Innovative Medicine Initiative 6 (“BeTheCure”; contract number 115142–2 to C.J.) and by institutional fundings. J.Q. was supported by the Arthritis Foundation.

Abstract

Promising immunotherapeutic strategies are emerging to restore tolerance in autoimmune diseases by triggering an increase in the number and/or the function of endogenous regulatory T (Treg) cells, which actively control pathological immune responses. Evidence suggests a remarkable heterogeneity in peripheral Treg cells that warrants their better characterization in terms of phenotype and suppressive function, to determine which subset may be optimally suitable for a given clinical situation.

We found that repetitive injections of immature dendritic cells (DCs) expanded FoxP3-negative CD49b$^+$ Treg cells that displayed an effector memory phenotype. These expanded Treg cells were isolated *ex-vivo* for transcriptome analysis and found to contain multiple transcripts of the canonical Treg signature shared mainly by CD25$^+$ but also by other sub-phenotypes. We characterized the CD49b$^+$ Treg cell phenotype, underscoring its similarities with the CD25$^+$ Treg cell phenotype and highlighting some differential expression patterns for several markers, including LAG-3, KLRG1, CD103, ICOS, CTLA-4 and Granzyme B. Comparison of the CD25$^+$ and CD49b$^+$ Treg cells' suppressive mechanisms, *in vitro* and *in vivo*, revealed the latter's potent suppressive activity, which was partly dependent on IL-10 secretion. Altogether our results strongly suggest that expression of several canonical Treg cell markers and suppressive function could be FoxP3-independent, and underscore the therapeutic potential of IL-10 secreting CD49b$^+$ Treg cells in arthritis.

Introduction

Regulatory T (Treg) cells actively suppress pathological and physiological immune responses, thereby contributing to the maintenance of immunological self-tolerance and immune homeostasis. Their development occurs in the thymus as a result of high-avidity TCR interactions with self-Ags (1), and are called thymus-derived Treg (tTreg) cells. These Treg cell subset are characterized by a stable expression of the transcription factor forkhead box P3 (FoxP3) (2) and constitutive high-level expression of CD25 (IL-2 receptor α chain) and thus denoted as $CD4^+CD25^+FoxP3^+$ Treg cells. The severity of the autoimmune syndromes caused by deficiencies in FoxP3 - scurfy in mice and IPEX in humans - highlights its central role (reviewed in (3)). Treg cells also differentiate extrathymically from conventional T cells and this differentiation is strongly modulated by cytokines such as IL-2 and TGF-β (4-6). These Treg cells have been termed peripheral Treg (pTreg) and several Ag-induced pTreg cell populations, with IL-10 based regulatory activity, appear to have critical *in vivo* functions (7-9). Several experimental tolerogenic settings have been shown to drive or increase expansion/differentiation of pTreg cells *in vivo*; these include chronic activation and sub-immunogenic Ag presentation (10-12), exposure to orally administered agonist peptides (13, 14), lymphopenia-driven homeostatic expansion (15-17) and use of small molecular weight compounds such as retinoic acid and histone deacetylase inhibitors (18, 19).

Alternative strategies to promote *in vivo* generation of stable pTreg cells use the tolerogenic properties of immature dendritic cells (DCs). Indeed, DC-based therapy has been proposed to restore tolerance in the context of several autoimmune diseases (20-22). The two main strategies developed are the direct targeting of antigens to DEC-205^+ steady state DCs (11, 23-26) and the repetitive injection of

tolerogenic DCs (27-29). We have previously demonstrated that repetitive injection of immature and semi-mature DCs can prevent adverse clinical outcome and protect mice from experimental collagen-induced arthritis (CIA) (30, 31). This protection was associated with the expansion of a particular FoxP3-negative $CD4^+$ Treg cell population characterized by the expression of CD49b (the alpha2 subunit of the adhesion molecule VLA-2) which specifically binds to collagens I, II and X (30). These induced $CD49b^+$ Treg cells, which secrete high levels of IL-4 and IL-10, displayed strong immunosuppressive properties *in vivo,* improving established CIA and attenuating delayed type hypersensitivity reactions (32, 33). Similarly, Benoist and Mathis' group demonstrated that $CD4^+CD49b^+$ Treg cells, present in naïve mice, were more efficient in suppressing the onset of diabetes than $CD4^+CD25^+$ Treg cells (34). As with the cell population we described, these cells' effect was IL-4 and IL-10 dependent. Recently, Gagliani *et al.* showed that CD49b and the lymphocyte activation gene 3 (LAG-3) define the IL-10-producing FoxP3-negative T regulatory type 1 cells (35).

Altogether these data reveal a remarkable heterogeneity in pTreg cell populations and define the CD49b molecule as a relevant marker for specific Treg cell subsets. Interestingly, recent studies challenged the notion that FoxP3 expression is uniquely responsible for all aspects of the transcriptional signature of $CD4^+CD25^+$ Treg cells and showed that FoxP3-independent epigenetic changes are required for Treg cell function (36, 37). These results underscore the need to better characterize the non-classical $CD49b^+$ induced Treg cells, which are mainly FoxP3-negative. We therefore investigated their suppressive mechanism *in vivo* and compared it with that of $CD25^+$ Treg cells in order to determine their respective therapeutic capacities.

Materials and Methods

Mice

DBA/1 mice were obtained from Harlan Laboratories and were bred in our own animal facility. Transgenic mice carrying the rearranged Vα11.1 and Vβ8.2 TCR chain genes isolated from a collagen-type II (Col II)-specific T cell hybridoma were kindly provided by R. Toes (LUMC, Leiden) with the approval of W. Ladiges. C57BL/6 wild type and C57BL/6 IL10$^{-/-}$ knockout mice (KO) were obtained from Janvier (B6.129P2-IL10^{tm1Cgn}/J) and were maintained in our animal facility under specific pathogen free conditions in isolated ventilated cages. Experimental groups were obtained by crossing heterozygous mice to obtain IL10-KO and wild type littermates with the same genetic background. Experiments were performed in accordance with national guidelines and approved by the Ethics committee for Animal Research of Languedoc-Roussillon (CEEA-LR-1067) and French Health Authorities (C34-172-36).

DC generation and injections

DCs were generated as previously described (30). Briefly, bone marrow cells were harvested from the femur and tibiae of mice and washed in RPMI following red blood cells lysis. T and B cells were depleted using mouse pan T and pan B Dynabeads® (Dynal) and monocytes were removed by 4h plate adhesion. The remaining cells were cultured in complete medium (RPMI 1640 supplemented with 5% FCS, 2mM L-glutamine, 5 x 10^{-5} M β-mercaptoethanol, 100U/ml penicillin, 100 µg/ml streptomycin, essential amino acids and 1 mM sodium pyruvate) with 1,000 IU/ml of rmGM-CSF (R&D Systems) and 1,000 IU/ml of rmIL-4 (R&D Systems) at 5 x 10^5 cells/ml in 24-well plates. Culture medium was renewed at days 2 and 4. For *in vivo* experiments, DCs were harvested at day 7. Syngeneic DBA/1, IL-10 KO or wild type littermates

were injected i.p. with 0.5 x 10^6 DCs in 100 µl PBS, 7, 5 and 3 days before euthanasia for splenic T cell purification.

Antibodies and FACS analysis

Spleens were harvested and single-cell suspensions were obtained by gentle passage through 70 µm nylon mesh filters (BD Biosciences). Following red blood cells lysis using ACK buffer, suspensions were pre-blocked using purified anti-CD16/32 Ab (2.4.G2) for 10 min. For intracellular cytokine staining, cells were stimulated during 48h at 37°C with anti-CD3/anti-CD28 antibody-coated Dynabeads (Dynal Biotech ASA, Oslo, Norway). During the last 4 hours of stimulation, 50 ng/ml of phorbol 12-myristate 13-acetate (PMA), 1 µg/ml of ionomycin and 10 µg/ml brefeldin A (Sigma-Aldrich, Zwijndrecht, The Netherlands) was added. Subsequently, cells were stained with surface antibodies (20 min, on ice). Cells were fixed using the eBioscience permeabilization kit according to the manufacturer's procedure and subsequently stained for intracellular markers. Data acquisition was performed on a Canto II or LSR Fortessa flow cytometer (BD Biosciences, Mountain View, CA) and analyses were performed using FlowJo software.

Treg cell isolation and adoptive cell transfer experiments

Splenocytes from DC-vaccinated mice were recovered by filtration on cell strainer, washed and then $CD4^+$ T cells purified by negative selection using Dynabeads. CD4 T cells were stained with anti-CD4, anti-CD49b and anti-CD25 conjugated antibodies and cell sorting was performed on FACSAria (MRI platform Montpellier, Fig.S1). FACS-sorted $CD4^+CD25^{+/-}CD49b^+$ T cells (purity >95 ± 2%), $CD4^+CD25^+CD49b^-$ (purity >96 ± 1%) or $CD4^+CD25^-CD49b^-$ T cells (purity >96 ± 1%), herein called

CD49b$^+$, CD25$^+$ and CD4$^+$ cells, respectively, were washed and 1.5 x 10^5 cells were injected i.v. in the tail vein of CIA mice or were used for subsequent analyses.

Gene Chip hybridization and data analysis.

Total RNA from CD4$^+$, CD25$^+$ and CD49b$^+$ T cells isolated from DC-injected mice and non-injected mice (CD4$^+$ only) were prepared using QIAGEN RNeasy Mini kit (QIAGEN). To reduce variability, we pooled cells from multiple mice (n>10) for cell-sorting, and three replicates were generated for CD25$^+$ and CD49b$^+$ cell groups as well as two replicates for CD4$^+$ cells isolated from DC-injected and non-injected mice. All gene-expression profiles were obtained from highly purified FACS-sorted T cell populations (MRI platform Montpellier). RNA was amplified, labeled, and hybridized (IVT Express, Affymetrix) to Affymetrix M430 PM Array Strips that cover almost all known murine genes. Affymetrix microarrays were processed at the Microarray Core Facility located at the IRMB institute. All chip data were uploaded to NCBI Gene Expression Omnibus (accession number is GSE68621, http://www.ncbi.nlm.nih.gov/geo/query/acc.cgi?acc=GSE68621) and are publicly available. Microarray data were analyzed according to a previously described procedure (38), to define the baseline average signal using the transcriptional profile of CD4$^+$ cells isolated from non-injected mice, and to calculate the differential expression variation using the transcriptional profiles of CD4$^+$, CD25$^+$ and CD49b$^+$ T cells isolated from DC-injected mice. To perform a robust analysis of the differentially expressed genes, we used the distribution of the number of differentially expressed transcripts to determine the optimal threshold for both the co-occurrence rate and the transcript expression variation (expression variation $\geq$1.15 and occurrence of 4/4 for CD4$^+$ and 6/6 for CD25$^+$ and CD49b$^+$) (39).

In vitro suppressive experiments

CFSE-labeled CD4 effector T cells (10^5) were cultured with titrated numbers of either FACS-sorted Treg cells or unlabeled-T effector cells in the presence of irradiated allogenic splenocytes (5 x 10^5) and 2-5 µg/ml of anti-CD3ε mAb (145-2C11). After 4 days of culture, proliferation of effector T cells was assessed by FACS. Data were analyzed using FlowJo software.

Collagen-induced arthritis (CIA) induction and evaluation

Male 9-12 week-old mice were immunized at the base of the tail with 100 µg of bovine or chicken Collagen type II (Col II) (MD biosciences) emulsified in CFA (Pierce, complemented to 4mg/ml with Mycobacterium tuberculosis H37RA) for DBA/1 or C57BL/6, respectively. To boost immunization, C57BL/6 mice received an i.v. injection of one million chicken Col II (2µg/ml)-loaded mature DCs on day 0. On day 21, DBA/1 or C57BL/6 mice received a booster immunization at the base of the tail with 100 µg of bovine Col II emulsified in IFA or chicken Col II emulsified in CFA, respectively. Mice were i.v. injected with the FACS-sorted Treg cells on day 28. From day 21, the thickness of each hind paw was measured 3 times a week with a caliper, and the severity of arthritis was graded according to the clinical scale previously described (40) with some modifications. Ankylosis was graded (score 5) and number of inflamed digits was also added to obtain a maximal score of 10 per paw and 40 per mouse. Clinical scores are represented as means ± SEM on a given day.

Cytokine secretion profile

Supernatants of FACS-sorted T cells (100,000 cells/well) were harvested 48 hours following *in vitro* stimulation and stored at -20°C until tested for the presence of murine IFN-γ, IL-10, IL-4, IL-5, and IL-13. All these cytokines were quantified by ELISA kits according to the manufacturer recommendations (R&D Systems).

Th1 or Th2 polarization of T cells

For *in vitro* differentiation, naïve OVA-specific $CD4^+$ T cells from DO11.10 transgenic mice were cultured during 3 days in Th1 (rIL-12, 10 ng/ml + anti IL-4 antibody, 5 µg/ml) or Th2 (rIL-4, 10 ng/ml + anti-IFN-γ antibody, 1.25 µg/ml) polarizing conditions with irradiated splenocytes in the presence of OVA peptide (1µg/ml) kindly provided by A. Chavanieu.

Statistics

Data are presented as mean ± SEM and significance was determined using GraphPad Prism software (GraphPad Software). Depending on the distribution of the data, parametric or non-parametric tests with appropriate comparisons were used to compare groups. A one-way or repeated two-way ANOVA with a post hoc multiple comparison test were used when more than two groups were compared.

Results

DC-induced CD49b cells display an effector memory phenotype

As we previously published (30, 32) and as clearly shown in figure S1, repetitive injections of immature DCs significantly induced $CD4^+CD49b^+$ cells (from 5 ± 0.2% to 9 ± 0.4%, $p<0.0001$) without modifying $CD4^+CD25^+$ cell frequencies (12 ± 0.2% to 12 ± 0.1%, NS; Fig. S1B). In naïve mice the $CD4^+CD49b^+$ cells are a heterogeneous population containing $FoxP3^+$ cells (57 ± 2%) and activated $CD25^+FoxP3^{neg}$ cells (7 ± 0.4%). After repeated DC injection, the expanded $CD4^+CD49b^+$ population showed a significant decrease in the percentage of FoxP3 expressing cells (24 ± 1%, $p<0.0001$; Fig. S1B) and a significant increase in the percentage of $CD25^{neg}FoxP3^{neg}$ cells (69 ± 0.9%, $p<0.0001$). These results demonstrate that the induced $CD49b^+$ cells were mostly $CD25^{neg}$ and $FoxP3^{neg}$. Although the frequency of $CD4^+CD25^+$ cells did not significantly change after repeated DC injection, we observed a slight increase in the frequency of these cells expressing FoxP3 (67 ± 1% to 76 ± 2%, $p<0.0001$). As shown in figure S1A, the analyzed populations were gated as $CD4^+CD49b^+CD25^{+/-}$, $CD4^+CD25^+$ and $CD4^+CD25^{neg}CD49b^{neg}$ cells and hereafter referred to as gated CD49b, CD25 and CD4 cells, respectively. The same gating strategy was used to sort the three populations.

To better characterize the DC-induced $CD49b^+$ cells, we compared their cell surface phenotype with those of $CD25^+$ and $CD4^+$ cells. We first compared the frequency of naïve T cells (defined as $CD44^{low}CD62L^{high}$) and effector memory T cells ($CD44^{high}CD62L^{low}$) within the gated CD4, CD25 and CD49b cell populations in non-injected and DC-injected mice (Fig. 1A lower right and upper left quadrant, respectively). The percentage of naïve T cells (Fig. 1B, top panels) was considerably

lower both in the $CD25^+$ (44 ± 1%) and $CD49b^+$ (26 ± 1%) cell populations, than in the $CD4^+$ cell population (65 ± 1%) of non-injected mice. Concomitantly, the percentages of effector memory T cells (Fig. 1B, bottom panels) were found to be higher in the $CD49b^+$ cell population (48 ± 0.5%) than in the $CD25^+$ and $CD4^+$ cell populations (25 ± 1% and 16%± 1%, respectively) of non-injected mice. Following DC-vaccination, we observed a slight but significant decrease in the percentage of cells with a naïve phenotype within the $CD25^+$ cell population (44 ± 1% and 36 ± 1%, $p<0.05$) and more importantly within the $CD49b^+$ cell population (26 ± 1% to 10 ± 1%, $p<0.0001$). These significant decreases in cells with naïve phenotype were associated with significant increases in cells with effector memory phenotype in the $CD49b^+$ (48 ± 0.5% to 66 ± 2%, $p<0.0001$) and to a lesser extent the $CD25^+$ (25 ± 1% to 33 ± 1%, $p<0.05$) cell populations. These data demonstrate that the $CD49b^+$ T cell population induced by DC vaccination clearly displayed an effector memory phenotype whereas the $CD25^+$ T cells phenotype was less impacted.

The transcriptional profiles of $CD49b^+$ T cells contain multiple transcripts of the canonical Treg cell signature shared either by $CD25^+$ or other Treg sub-phenotypes

To identify the genes differentially expressed by $CD25^+$ and $CD49b^+$, defined as prototypical Treg transcripts, we compared the gene expression patterns of highly purified T cells. The gating strategy and purity of FACS-sorted $CD49b^+$, $CD25^+$ and $CD4^+$ populations are given in Supplemental Figure 1. We determined the differential transcriptional profiles associated with the DC-vaccination protocol by comparative analysis of the FACS-sorted $CD4^+$ cells isolated from non-injected and DC-injected mice. The transcriptional profiles of DC-induced $CD25^+$ and $CD49b^+$ included both

the transcriptional profile associated with the $CD4^+$ cell subset and the DC-vaccination induced transcripts. To focus our analysis only on $CD49b^+$ and $CD25^+$ specific transcripts, we removed the transcripts associated with DC vaccination found in $CD4^+$. We were therefore able to compare these $CD25^+$ and $CD49b^+$ differential gene expression profiles with the canonical Treg cell expression signature consisting of 603 probe sets (16, 26, 37). These 603 probe sets defined by Hill *et al.*, correspond to 431 transcripts (138 down-regulated and 293 up-regulated) that revealed a mean probe set redundancy of 1.4 in their study. In our study, the precise and robust analysis of the differentially expressed transcripts is underscored by the mean global score for probe redundancy of 2.0. We found 79 differentially expressed transcripts in the $CD49b^+$ cells (18 down-regulated and 61 up-regulated) and 128 differentially expressed transcripts in the $CD25^+$ cells (28 down-regulated and 100 up-regulated) all in common with the canonical Treg signature, with similar modulation described by Hill *et al*. (Fig. 2A). Interestingly the $CD25^+$ and $CD49b^+$ cell populations shared 59 differentially expressed transcripts (11 down-regulated and 48 up-regulated) (Fig 2B), corresponding to 74.6% of the differentially expressed transcripts found in $CD49b^+$, therefore underscoring the similarities between $CD49b^+$ and $CD25^+$ Treg cells. Similar transcriptional expression variations were observed between $CD49b^+$ and $CD25^+$ Treg cells with similar modulations to those described by Hill *et al*. The common transcriptional pattern between $CD49b^+$ and $CD25^+$ contained several prototypical Treg transcripts, including *Itgae*, *Klrg1, Nrp1*, *Gzmb, Ebi3, Entpd1, Dusp4*, *Socs2*, *Ahr*, *Swap70.*

We also found that each cell population uniquely expressed several canonical Treg cell signature transcripts: 69 for $CD25^+$ (17 down-regulated and 52 up-regulated) and 20 for $CD49b^+$ (7 down-regulated and 13 up-regulated) (Fig. 2A and

Fig. S2). Interestingly among the transcripts specific for CD49b$^+$, we found *AcoT7, LXN, 5830474E16Rik, Gpr34, Pros1 and Ndrg1*. These transcripts have previously been described as differentially expressed in conventional Treg cells isolated from spleen, and highly expressed in CD103$^+$ and KLRG1$^+$ Treg cells (26). Altogether, our results demonstrate that the CD49b$^+$ transcriptional signature contains prototypical Treg cell transcripts shared by either CD25$^+$ or other Treg cell sub-phenotypes.

CD49b$^+$ Treg cells express several canonical markers of CD25$^+$FoxP3$^+$ Treg cells.

To further characterize and compare the phenotypes of the DC-induced CD49b$^+$ and CD25$^+$ cells isolated from the same DC-vaccinated mice, we performed 6-10 colors cytometric analyses. We showed that, despite weakly expressing CD25 and the master regulator transcription factor FoxP3 (Fig. S1), CD49b$^+$ cells express markers commonly used to characterize CD25$^+$FoxP3$^+$ Treg cells, including CD103, KLRG1, CTLA-4, latency associated peptide (LAP) and glucocorticoid-induced TNFR family related gene (GITR) (Fig. 3). Interestingly, CD49b$^+$ cells also expressed programmed cell death-1 (PD1), shown to play an important role in pTreg cell induction and function (41), although at a lower level than that in CD25$^+$ cells (Fig. 3A). Moreover, expression of LAG-3, KLRG1 and CD103 molecules was in contrast significantly higher in CD49b$^+$ than in CD25$^+$ cells (Fig. 3A). Within the CD49b$^+$ cell population, we noted that LAG-3 expression was mostly restricted to the FoxP3^{neg} cells, whereas KLRG1 and CD103 expressions were found in both FoxP3$^+$ and FoxP3^{neg} cells.

Several molecules sustaining the Treg cell suppressive function are known to be highly expressed following activation. As CD25 and CD49b expressions are also

modulated following activation, we first purified the T cells from DC-vaccinated mice by FACS-sorting them (Fig. S1) and the three resulting populations were analyzed 48 hours following *in vitro* stimulation. Phenotypic analysis of activated T cells clearly showed that all T cells acquired CD25 expression, and that half of the $CD25^+$ Treg cells were $FoxP3^+$ compared to less than 4% of the $CD49b^+$ Treg cells (Fig. 3B). Interestingly, compared to the $CD25^+$ T cell population, that of the $CD49b^+$ T cells displayed higher percentages or mean fluorescence intensity (MFI) of several markers commonly expressed by Treg cells. These markers included Granzyme B (GrB), GITR, inducible T-cell costimulator (ICOS), LAP and IL-10 in terms of percentages, and CTLA-4 for MFI. We narrowed our focus down to effector mechanisms by comparing the phenotype of IL-10 secreting T cells (gated within the $CD49b^+$ cell population) with that of $FoxP3^+$ cells (gated within the $CD25^+$ cell population) (Fig. S3). Interestingly, the $FoxP3^+$ cell sub-population displayed a higher percentage of cells expressing LAP than did the IL-10 secreting sub-population (31 ± 8% versus 10 ± 0.5% respectively, p=0.008). Conversely, GITR (96 ± 0.5% versus 78 ± 3%, p= 0.026), CTLA-4 (97 ± 0.1% versus 84 ± 5%, p= 0.02) and GrB (31 ± 8% versus 2.5 ± 0.3%, p=0.010) were more frequently expressed among the IL-10 secreting $CD49b^+$ Treg cells than in the $FoxP3^+CD25^+$ cell sub-population. These results suggest that, besides IL-10, these three molecules could play an important role in the $CD49b^+$ suppressive function (Fig. S3).

Peripherally induced $CD49b^+$ cells express Neuropilin-1 without co-expressing Helios.

Neuropilin-1 (Nrp-1) was proposed as a Treg cell surface marker in 2004 (42) and its coordinated expression along with Helios, an Ikaros family transcription factor,

was more recently suggested for use in distinguishing thymic derived from inducible Foxp3^{+}CD25^{+} Treg cells (43-46). Indeed, pTreg cell populations generated *in vivo* displayed reduced Nrp-1 expression compared with tTreg cells, indicating Nrp-1 as a tTreg specific marker (26). As previously published for NOD and C57BL/6 mice (43), we showed in DBA/1 mice that the majority of CD25^{+} cells express concurrently Nrp-1 and Helios (56 ± 3%) (Fig. 4). Interestingly, Nrp-1 expression was high (58 ± 1%) but Helios expression was significantly lower (15 ± 1%) in CD49b^{+} cells. Moreover, we observed that CD49b^{+}Helios^{+} cells co-expressed Nrp-1^{+} and FoxP3^{+} suggesting that among the CD49b^{+} cell population, almost 20% of cells could be considered as natural tTreg cells based on the concomitant expression of Helios, Nrp-1 and FoxP3 (Fig.4). Altogether, our results show that induced FoxP3^{neg}CD49b^{+} Treg cells are positive for Nrp-1 but do not co-express Helios, as expected for induced pTreg cells.

Peripheral induced CD49b cells express Th1- and Th2-specific transcriptional factors and cytokines

Recent evidence suggests that the capacity of Treg cells to control polarized settings can be associated with the expression of specific transcription factors, such as T-bet, interferon regulatory factor 4 (IRF4) and STAT3 to control Th1, Th2 and Th17 responses respectively (47-49). Treg cells expressing these transcription factors can partially mimic the phenotype of the effector T cells, providing them with particular homing, survival, or functional properties (50). It has been demonstrated that 25% of FoxP3^{+} compared to only 5% of FoxP3^{neg} Treg cells isolated from spleen express the canonical Th2 transcription factor Gata3 (51). These authors showed that the expression of Gata3 controlled unbalanced polarization and inflammatory cytokine production in Treg cells, and that it was required for the maintenance of

370 FoxP3 high level expression and promoted the accumulation of Treg cells at inflamed
371 sites (51). In our study in DBA/1 mice, we observed Gata3 expression in 8 ± 1% of
372 the $CD25^+$ cells and in 47 ± 2% of the $CD49b^+$ cell population (Fig. 5A). Furthermore,
373 we observed that only the DC-induced $CD49b^+$ cells displayed a considerable
374 proportion of double positive staining for T-bet and Gata3 (25 ± 1.5%), in contrast
375 with the $CD4^+$ and $CD25^+$ cells (2 ± 0.2% for both populations) (Fig. 5A, right panel).
376 This DC-induced increase in the number of $CD49b^+$ cells expressing both T-bet and
377 Gata3 was statistically significant (25 ± 1.5% versus 2 ± 0.2%, $p<0.0001$).

378 C-Maf was the first Th2-specific transcription factor identified and has been
379 shown to play a critical role in trans-activating IL-4 and IL-10 expression during Th17
380 polarization. The ligand-activated transcription factor aryl hydrocarbon receptor
381 (AhR), like the proto-oncogene Maf, was shown to be strongly induced during Tr1 cell
382 differentiation with similarly high levels of expression found in both Tr1 and Th17 cells
383 (52). We thus evaluated the expression of c-Maf and AhR in $CD49b^+$ cells and found
384 them in 53 ± 2% and 82 ± 1% respectively, compared to in only 38 ± 1% and 39 ± 2%
385 respectively of the $CD25^+$ population (Fig. 5B).

386 To further characterize the cytokine secretion profile we quantified the level of
387 cytokine secretion in the supernatant of highly purified FACS-sorted cells following
388 their *in vitro* activation. Besides the high level of IL-10 secretion (19 ± 7 ng/ml), we
389 measured significantly elevated secretion levels of other type 2 cytokines, including
390 IL-4 (10 ± 2 ng/ml), IL-5 (18 ± 2 ng/ml) and IL-13 (31 ± 0.5 ng/ml), as well as a
391 relatively high amount of IFN-γ (3 ± 1 ng/ml) in the supernatant of the $CD49b^+$ T cell
392 population. These results revealed an obvious type 2 dominant cytokine profile for
393 the $CD49b^+$ Treg cells and underscored their dissimilarity with Tr1 cells, which
394 secrete high levels of IL-10 without concomitant secretion of IL-4 (40, 53).

Polyclonal and Ag-specific CD49b$^+$ Treg cells have potent *in vitro* and *in vivo* suppressive capacities

We compared the *in vitro* potential of CD49b$^+$ and CD25$^+$ Treg cells to functionally suppress the proliferation of CD4$^+$ T cells by co-cultivating Treg and responder cell populations stimulated by a polyclonal T cell receptor stimulator (anti-CD3 mAb) and in the presence of antigen-presenting cells. Addition of CD49b$^+$ or CD25$^+$ Treg cells reduced the proliferation, as measured by the CFSE dilution, in a dose-dependent manner thus confirming their potent *in vitro* suppressive capacities (Fig 6A).

We previously demonstrated the *in vivo* therapeutic potential of CD49b$^+$ Treg cells to protect against (30) as well as to improve the condition of established arthritis (32). To further investigate the therapeutic potential of CD49b$^+$ Treg cells, we compared their protective effect with that of CD25$^+$ Treg cells isolated from the same DBA/1 mice and with CD49b$^+$ Treg cells isolated from Col II-specific T cell transgenic mice (TBC). We repeatedly injected syngeneic mice intraperitoneally with 0.5 x 10^6 DCs the week before their euthanasia. CD4$^+$ T cells were pre-purified and the Treg cells were FACS-sorted to obtain >98% pure population. The FACS-sorted populations were adoptively transferred intravenously into collagen-induced arthritic (CIA) mice on day 28, at the onset of the clinical signs. In this experimental setting that mimics the clinical situation, we observed a similar decrease of arthritis severity in mice injected with either of the polyclonal Treg cells, CD49b$^+$ or CD25$^+$, isolated from the same DBA/1 mouse, or with the antigen-specific CD49b$^+$ Treg cells (CD49b TBC, Fig. 6B). Similar results were obtained in several independent experiments, and we performed robust statistical analyses using relative arthritic scores calculated

using the mean of the PBS-treated mice as 100% disease severity for each experiment. We included in these experiments a control group of mice, which were injected with the $CD4^+$ cell population. As shown in figure 6C, injection of polyclonal $CD49b^+$ Treg cells markedly and significantly decreased the disease severity compared with PBS-treated or $CD4^+$-treated mice. We observed a tendency towards decreased disease severity after injection of the $CD25^+$ Treg cells or of the antigen-specific $CD49b^+$ Treg cells isolated from TBC mice, however these decreases were not significant. These results in the CIA experimental model suggest that the use of $CD49b^+$ Treg cells may represent the best therapeutic strategy, over the use of natural $CD25^+$ Treg cells.

Finally, to further investigate the *in vivo* suppressive mechanism, we performed similar adoptive transfer experiments with $CD49b^+$ Treg cells isolated from IL-10 KO mice. In this experimental setting, $CD49b^+$ Treg cells were isolated from IL-10 KO or wild-type littermates and injected on day 28 into arthritis-induced C57BL/6 mice. As clearly shown in figure 6D, injection of $CD49b^+$ isolated from wild-type littermates significantly protected mice from arthritis whereas IL-10 deficient $CD49b^+$ Treg cells were less protective. These results underscore the partial involvement of IL-10 secretion in the $CD49b^+$ Treg protective effect and suggest that alternative mechanisms might be important for their *in vivo* suppressive function.

Discussion

The discovery that Treg cells can control autoimmune inflammatory responses has led to great enthusiasm for their clinical application in autoimmune diseases such as rheumatoid arthritis (RA). The hope is that the impaired Treg cell differentiation may be corrected by adoptive transfer of *in vitro*-generated autologous Treg cells or by immunotherapeutic strategies triggering an increase in the number and/or an improved functioning of endogenous Treg cells.

In vitro generation of autologous Treg cells could be a treatment option for multiple autoimmune diseases, including experimental autoimmune encephalomyelitis, diabetes, colitis, and lupus (54-56). However, this approach is quite challenging because it is difficult to generate and/or expand Treg cells with specific Ag specificity, especially when the immunodominant epitopes are uncharacterized, such as in RA. Nevertheless, *in vitro* expansion of Col II-specific Tr1 cells isolated from RA patients was recently demonstrated (57). Pre-clinical proof-of-concept concerning the therapeutic potential of *in vitro* generated Col II-specific Tr1 cells has also been recently validated in two experimental models of arthritis (40). Altogether these results support the therapeutic use of ex-vivo expanded autologous Ag-specific Treg cells in RA.

However, some evidence suggests that Treg cells generated *in vitro* are phenotypically and functionally unstable, whereas those induced *in vivo* are epigenetically more stable and would lead to a longer-lasting therapeutic effect (4, 58, 59). The *in vivo*-induced Treg cells are usually Ag specific, which implies a likely more efficient effect in treating autoimmune diseases. In RA patients, TNF-α blocking antibodies have been described as an effective way to stimulate the induction of peripheral FoxP3$^+$ Treg cells, overcoming the impaired peripheral Treg cell

differentiation (60). For all these reasons, the development of strategies to promote *in vivo* generation of Ag-specific Treg cells appears crucial for the treatment of autoimmune diseases.

The aim of our study was to better characterize a particular sub-population of *in vivo*-induced CD49b$^+$ Treg cells. We demonstrated that this particular Treg cell subset expresses several canonical markers of Treg cells while being mostly negative for CD25 and FoxP3, which are routinely used to identify Treg cells. We first demonstrated that 30% of the Treg cell signature was found in the CD25$^+$ Treg cell specific expression profile. Indeed, the Treg cell canonical signature is a composite signature derived from Treg cells isolated from several lymphoid organs (37). This bulk of Treg cell sub-phenotypes could explain the lack of complete overlapping with the specific transcriptional profile of CD25$^+$ cells in our study. A similar lack of complete overlapping has previously been observed when comparing the transcriptional profile of converted FoxP3$^+$ Treg cells with the canonical Treg cell signature (26). Interestingly, the induced CD49b$^+$ Treg cells shared a transcriptional profile common to CD25$^+$ Treg cells and the canonical Treg cell signature. We showed that 75% of the differentially expressed transcripts found in CD49b$^+$ T cells were common with those found in CD25$^+$ T cells, underscoring the similarities between CD49b$^+$ and CD25$^+$ Treg cells. Indeed, we demonstrated that these cells share a common signature of 59 prototypical Treg cell transcripts including effector molecules and transcription factors. Several transcripts from this common signature have been proposed as promising candidates to specifically discriminate between Ag-induced and homeostatically converted Treg cells, including Itgae, Ctla4, Entpd1 (CD39), Ebi3 (a component of IL35), Irf4, αEβ7 (CD103) and Klrg1 (a member of the killer cell lectin-like receptor family). The CD49b$^+$ Treg cell transcriptional profile also

contained several specific transcripts in common with the canonical Treg signature. These results suggest an overlap of the transcriptional profile of CD49b$^+$ Treg cells with several other Treg sub-phenotypes.

We validated by FACS analyses the common expression of several markers between CD25$^+$ and CD49b$^+$ cells that were differentially expressed compared with CD4$^+$. Among these markers, CD49b and KLRG1, both considered as NK cell markers and minimally expressed on conventional CD4$^+$ T cells, were previously observed in an extrathymically derived subset of CD4$^+$CD25$^+$FoxP3$^+$ Treg cells (61). Within the sub-population of CD25$^+$FoxP3$^+$ Treg cells in the spleen, KLRG1$^+$ Treg cells were previously shown to display a more activated phenotype (CD69$^+$CD62L^{low}CD103$^+$CD44^{high}) than KLRG1^{neg} Treg cells. Furthermore, cell-surface staining of homeostatically converted FoxP3$^+$ cells revealed them as uniformly CD103$^+$, an excellent marker for identifying *in vivo*–activated FoxP3$^+$CD4$^+$ Treg cells, and that 50% of the cells expressed KLRG1 (26). We showed that the two markers, KLRG1 and CD103, were expressed on CD49b$^+$ and CD25$^+$ cells and, as previously observed for the CD4$^+$CD25$^+$FoxP3$^+$ Treg cells, were associated with an activated phenotype for the CD49b cells. Similarly, Nrp-1 was previously described on a population of activated/memory FoxP3^{neg}Nrp-1$^+$ in secondary lymphoid organs and inflamed tissues, which could imply that the expression of Nrp-1 is associated with the CD49b$^+$ activated/memory phenotype. Finally, the lack of concomitant expression of Nrp-1 and Helios as well as their effector/memory phenotype confirm the peripheral origin of these cells.

Initially characterized as a Th2 specific cytokine, IL-10 has since been found expressed by almost all CD4$^+$ T cells, including CD25$^+$FoxP3$^+$ Treg cells and Tr1 cells, but also Th1, Th2 and Th17 cells, in order to promote immune homeostasis.

Previous mouse studies have described the collaborative actions of c-Maf with AhR and the ICOS receptor ligation that drive IL-10 expression and promote Tr1 differentiation (52, 62). We demonstrated in this study that the CD49b$^+$ Treg cells highly express these three molecules suggesting that, similarly to Tr1 cells, several transcriptional pathways, associated with high secretion of IL-10, are activated. CD49b$^+$ cells are also positive for the Th2 specific transcription factor Gata3 and 30% of the cells are double positive for T-bet and Gata3 with concomitant secretion of IFN-γ and Th2 cytokines. The co-expression of T-bet and Gata3 has been previously observed *in vivo* following viral infection and this hybrid phenotype appeared to be stable (63). Altogether our results suggest that the CD49b$^+$ cells display a balanced Th2/Th1 phenotype that could endow them with specific properties to better control effector T cell responses.

Other similarities and differences between IL-10-secreting CD49b$^+$ Treg cells and Tr1 cells can be discussed. Co-expression of CD49b and LAG-3 has been recently proposed as specific for Tr1 cells (35). In our experimental setting, only 5 to 10% of CD49b$^+$ Treg cells were positive for LAG-3 before *in vitro* activation and interestingly CD49b$^+$LAG-3$^+$ cells are mostly FoxP3 negative cells like Tr1 cells. Furthermore Tr1 cells are reported to be induced at mucosal sites in response to antigen stimulation in the presence of IL-10. We observed that IL-10 deficient DCs promoted IL-10 secreting CD49b$^+$ Treg cell expansion in several lymphoid organs of wild type animals suggesting that, in contrast to Tr1 cells (64), the IL-10 secretion by DCs is dispensable for the expansion of CD49b$^+$ (P. Louis-Plence, unpublished data). Altogether our results suggest that the CD49b$^+$ Treg cells constitute a Treg sub-phenotype that shares similarities with the CD25$^+$ Treg cells as well as with the Tr1

539 cells, and should be considered alongside other sub-phenotypes as homeostatically
540 converted or antigen-induced.

541 Here we have investigated the suppressive function of $CD25^+$ and $CD49b^+$
542 Treg cell populations *in vitro* and *in vivo*, in the experimental model of CIA. *In vitro,*
543 both Treg cell populations similarly suppressed the T cell proliferation. To compare
544 their therapeutic potential in CIA, we injected $CD25^+$, polyclonal $CD49b^+$ or Col II-
545 specific $CD49b^+$ Treg cells at the onset of clinical signs of arthritis. As previously
546 described (32), we demonstrated a significant reduction of these clinical signs
547 following injection of polyclonal $CD49b^+$ Treg cells. Although not significant, we also
548 observed decreased clinical signs following injection of $CD25^+$ or Col II-specific
549 $CD49b^+$ Treg cells. Our results suggest that following their activation by self-Ag(s),
550 the $CD49b^+$ regulatory T cells display a potent bystander suppressive function and as
551 polyclonal *in vivo*-expanded Treg cells, they could be a better alternative to classical
552 Treg cells for arthritis treatment. The suppressive function of $CD49b^+$ Treg cells was
553 found to be partially dependent on IL-10 secretion. Moreover expression of several
554 canonical Treg markers, implicated in the Treg suppressive function, suggests that
555 other molecules might also play a role in the CD49b suppressive activity. Indeed, GrB
556 and CTLA-4 have been shown to play a crucial role in the suppressive function of
557 conventional $CD25^+FoxP3^+$ Treg cells and thus might also play an important role in
558 the suppressive function of $CD49b^+$ Treg cells. Furthermore, CD103 expression could
559 also be implicated in their suppressive function as its expression was shown to be
560 responsible for the retention of Treg cells in inflamed tissue by interaction with its
561 ligand E-cadherin (65, 66). Finally, expression of the alpha2 integrin CD49b itself,
562 could also be important for their function since it was demonstrated that this integrin
563 is required for the migration of memory CD4 T-cell precursors into their survival

niches of the bone marrow (67). Since VLA-2 also binds collagen II, expression of CD49b could provide Treg cells with particular homing, survival, or more potent suppressive function in the context of arthritis since collagen II is expressed by the damaged cartilage.

In this study, we have provided an in-depth characterization of the CD49b$^+$ Treg cells, underscoring their similarities with other Treg sub-phenotypes and highlighting specific expression patterns for several markers including ICOS, CTLA-4 and GrB. The expression of these canonical Treg markers strongly supports the notion that several suppressive mechanisms could be FoxP3-independent. Their potent suppressive activity *in vivo*, higher than that of the classical CD25$^+$ Treg cells, underscores the need to select appropriate Treg subsets for a given clinical application and supports their therapeutic application in RA.

Acknowledgments

We thank Myriam Boyer and Christophe Duperray (Montpellier RIO Imaging platform) for performing cell-sorting experiments with the FACSAria and the ECELLFRANCE national infrastructure for providing the LSR Fortessa cytometer. We also thank Véronique Pantesco for gene-chip hybridization and the animal facility staff located at the INM institute in Montpellier (RAM network) for their expert care of the mice colonies.

References

1. Klein, L., and K. Jovanovic. Regulatory T cell lineage commitment in the thymus. *Semin Immunol* 23:401-409.
2. Wing, K., and S. Sakaguchi. Regulatory T cells exert checks and balances on self tolerance and autoimmunity. *Nat Immunol* 11:7-13.
3. Ziegler, S. F. 2006. FOXP3: of mice and men. *Annu Rev Immunol* 24:209-226.

4. Chen, Q., Y. C. Kim, A. Laurence, G. A. Punkosdy, and E. M. Shevach. 2003. IL-2 controls the stability of Foxp3 expression in TGF-beta-induced Foxp3+ T cells in vivo. *J Immunol* 186:6329-6337.
5. Curotto de Lafaille, M. A., and J. J. Lafaille. 2009. Natural and adaptive foxp3+ regulatory T cells: more of the same or a division of labor? *Immunity* 30:626-635.
6. Zheng, S. G., J. Wang, P. Wang, J. D. Gray, and D. A. Horwitz. 2007. IL-2 is essential for TGF-beta to convert naive CD4+CD25- cells to CD25+Foxp3+ regulatory T cells and for expansion of these cells. *J Immunol* 178:2018-2027.
7. O'Garra, A., and P. Vieira. 2004. Regulatory T cells and mechanisms of immune system control. *Nat Med* 10:801-805.
8. Hawrylowicz, C. M., and A. O'Garra. 2005. Potential role of interleukin-10-secreting regulatory T cells in allergy and asthma. *Nat Rev Immunol* 5:271-283.
9. Roncarolo, M. G., S. Gregori, M. Battaglia, R. Bacchetta, K. Fleischhauer, and M. K. Levings. 2006. Interleukin-10-secreting type 1 regulatory T cells in rodents and humans. *Immunol Rev* 212:28-50.
10. Verginis, P., K. A. McLaughlin, K. W. Wucherpfennig, H. von Boehmer, and I. Apostolou. 2008. Induction of antigen-specific regulatory T cells in wild-type mice: visualization and targets of suppression. *Proc Natl Acad Sci U S A* 105:3479-3484.
11. Kretschmer, K., I. Apostolou, D. Hawiger, K. Khazaie, M. C. Nussenzweig, and H. von Boehmer. 2005. Inducing and expanding regulatory T cell populations by foreign antigen. *Nat Immunol* 6:1219-1227.
12. Apostolou, I., and H. von Boehmer. 2004. In vivo instruction of suppressor commitment in naive T cells. *J Exp Med* 199:1401-1408.
13. Mucida, D., N. Kutchukhidze, A. Erazo, M. Russo, J. J. Lafaille, and M. A. Curotto de Lafaille. 2005. Oral tolerance in the absence of naturally occurring Tregs. *J Clin Invest* 115:1923-1933.
14. Curotto de Lafaille, M. A., N. Kutchukhidze, S. Shen, Y. Ding, H. Yee, and J. J. Lafaille. 2008. Adaptive Foxp3+ regulatory T cell-dependent and -independent control of allergic inflammation. *Immunity* 29:114-126.
15. Knoechel, B., J. Lohr, E. Kahn, J. A. Bluestone, and A. K. Abbas. 2005. Sequential development of interleukin 2-dependent effector and regulatory T cells in response to endogenous systemic antigen. *J Exp Med* 202:1375-1386.
16. Haribhai, D., W. Lin, B. Edwards, J. Ziegelbauer, N. H. Salzman, M. R. Carlson, S. H. Li, P. M. Simpson, T. A. Chatila, and C. B. Williams. 2009. A central role for induced regulatory T cells in tolerance induction in experimental colitis. *J Immunol* 182:3461-3468.
17. Curotto de Lafaille, M. A., A. C. Lino, N. Kutchukhidze, and J. J. Lafaille. 2004. CD25- T cells generate CD25+Foxp3+ regulatory T cells by peripheral expansion. *J Immunol* 173:7259-7268.
18. Benson, M. J., K. Pino-Lagos, M. Rosemblatt, and R. J. Noelle. 2007. All-trans retinoic acid mediates enhanced T reg cell growth, differentiation, and gut homing in the face of high levels of co-stimulation. *J Exp Med* 204:1765-1774.
19. Edwards, A. J., and S. L. Pender. Histone deacetylase inhibitors and their potential role in inflammatory bowel diseases. *Biochem Soc Trans* 39:1092-1095.
20. Amodio, G., A. Mugione, A. M. Sanchez, P. Vigano, M. Candiani, E. Somigliana, M. G. Roncarolo, P. Panina-Bordignon, and S. Gregori. HLA-G expressing DC-10 and CD4(+) T cells accumulate in human decidua during pregnancy. *Hum Immunol* 74:406-411.

21. Gross, C. C., and H. Wiendl. Dendritic cell vaccination in autoimmune disease. *Curr Opin Rheumatol* 25:268-274.
22. Hilkens, C. M., J. D. Isaacs, and A. W. Thomson. 2010. Development of dendritic cell-based immunotherapy for autoimmunity. *Int Rev Immunol* 29:156-183.
23. Mahnke, K., Y. Qian, J. Knop, and A. H. Enk. 2003. Induction of CD4+/CD25+ regulatory T cells by targeting of antigens to immature dendritic cells. *Blood* 101:4862-4869.
24. Kretschmer, K., T. S. Heng, and H. von Boehmer. 2006. De novo production of antigen-specific suppressor cells in vivo. *Nat Protoc* 1:653-661.
25. Idoyaga, J., C. Fiorese, L. Zbytnuik, A. Lubkin, J. Miller, B. Malissen, D. Mucida, M. Merad, and R. M. Steinman. Specialized role of migratory dendritic cells in peripheral tolerance induction. *J Clin Invest* 123:844-854.
26. Feuerer, M., J. A. Hill, K. Kretschmer, H. von Boehmer, D. Mathis, and C. Benoist. 2010. Genomic definition of multiple ex vivo regulatory T cell subphenotypes. *Proc Natl Acad Sci U S A* 107:5919-5924.
27. Jonuleit, H., E. Schmitt, G. Schuler, J. Knop, and A. H. Enk. 2000. Induction of interleukin 10-producing, nonproliferating CD4(+) T cells with regulatory properties by repetitive stimulation with allogeneic immature human dendritic cells. *J Exp Med* 192:1213-1222.
28. Menges, M., S. Rossner, C. Voigtlander, H. Schindler, N. A. Kukutsch, C. Bogdan, K. Erb, G. Schuler, and M. B. Lutz. 2002. Repetitive injections of dendritic cells matured with tumor necrosis factor alpha induce antigen-specific protection of mice from autoimmunity. *J Exp Med* 195:15-21.
29. Petzold, C., J. Riewaldt, T. Koenig, S. Schallenberg, and K. Kretschmer. Dendritic cell-targeted pancreatic beta-cell antigen leads to conversion of self-reactive CD4(+) T cells into regulatory T cells and promotes immunotolerance in NOD mice. *Rev Diabet Stud* 7:47-61.
30. Charbonnier, L. M., L. M. van Duivenvoorde, F. Apparailly, C. Cantos, W. G. Han, D. Noel, C. Duperray, T. W. Huizinga, R. E. Toes, C. Jorgensen, and P. Louis-Plence. 2006. Immature dendritic cells suppress collagen-induced arthritis by in vivo expansion of CD49b+ regulatory T cells. *J Immunol* 177:3806-3813.
31. van Duivenvoorde, L. M., P. Louis-Plence, F. Apparailly, E. I. van der Voort, T. W. Huizinga, C. Jorgensen, and R. E. Toes. 2004. Antigen-specific immunomodulation of collagen-induced arthritis with tumor necrosis factor-stimulated dendritic cells. *Arthritis Rheum* 50:3354-3364.
32. Charbonnier, L. M., W. G. Han, J. Quentin, T. W. Huizinga, J. Zwerina, R. E. Toes, C. Jorgensen, and P. Louis-Plence. 2010. Adoptive transfer of IL-10-secreting CD4+CD49b+ regulatory T cells suppresses ongoing arthritis. *J Autoimmun* 34:390-399.
33. Han, W. G., E. I. van der Voort, H. el Bannoudi, P. Louis-Plence, T. W. Huizinga, and R. E. Toes. 2010. DX5(+)CD4(+) T cells modulate cytokine production by CD4(+) T cells towards IL-10 via the production of IL-4. *Eur J Immunol* 40:2731-2740.
34. Gonzalez, A., I. Andre-Schmutz, C. Carnaud, D. Mathis, and C. Benoist. 2001. Damage control, rather than unresponsiveness, effected by protective DX5+ T cells in autoimmune diabetes. *Nat Immunol* 2:1117-1125.
35. Gagliani, N., C. F. Magnani, S. Huber, M. E. Gianolini, M. Pala, P. Licona-Limon, B. Guo, D. R. Herbert, A. Bulfone, F. Trentini, C. Di Serio, R. Bacchetta, M. Andreani, L.

Brockmann, S. Gregori, R. A. Flavell, and M. G. Roncarolo. 2013. Coexpression of CD49b and LAG-3 identifies human and mouse T regulatory type 1 cells. *Nat Med* 19:739-746.

36. Ohkura, N., M. Hamaguchi, H. Morikawa, K. Sugimura, A. Tanaka, Y. Ito, M. Osaki, Y. Tanaka, R. Yamashita, N. Nakano, J. Huehn, H. J. Fehling, T. Sparwasser, K. Nakai, and S. Sakaguchi. T cell receptor stimulation-induced epigenetic changes and Foxp3 expression are independent and complementary events required for Treg cell development. *Immunity* 37:785-799.
37. Hill, J. A., M. Feuerer, K. Tash, S. Haxhinasto, J. Perez, R. Melamed, D. Mathis, and C. Benoist. 2007. Foxp3 transcription-factor-dependent and -independent regulation of the regulatory T cell transcriptional signature. *Immunity* 27:786-800.
38. Chuchana, P., D. Marchand, M. Nugoli, C. Rodriguez, N. Molinari, and J. A. Garcia-Sanz. 2007. An adaptation of the LMS method to determine expression variations in profiling data. *Nucleic Acids Res* 35:e71.
39. Chuchana, P., P. Holzmuller, F. Vezilier, D. Berthier, I. Chantal, D. Severac, J. L. Lemesre, G. Cuny, P. Nirde, and B. Bucheton. 2010. Intertwining threshold settings, biological data and database knowledge to optimize the selection of differentially expressed genes from microarray. *PLoS One* 5:e13518.
40. Asnagli, H., D. Martire, N. Belmonte, J. Quentin, H. Bastian, M. Boucard-Jourdin, P. B. Fall, A. L. Mausset-Bonnefont, A. Mantello-Moreau, S. Rouquier, I. Marchetti, C. Jorgensen, A. Foussat, and P. Louis-Plence. 2014. Type 1 regulatory T cells specific for collagen-type II as an efficient cell-based therapy in arthritis. *Arthritis Res Ther* 16:R115.
41. Francisco, L. M., V. H. Salinas, K. E. Brown, V. K. Vanguri, G. J. Freeman, V. K. Kuchroo, and A. H. Sharpe. 2009. PD-L1 regulates the development, maintenance, and function of induced regulatory T cells. *J Exp Med* 206:3015-3029.
42. Bruder, D., M. Probst-Kepper, A. M. Westendorf, R. Geffers, S. Beissert, K. Loser, H. von Boehmer, J. Buer, and W. Hansen. 2004. Neuropilin-1: a surface marker of regulatory T cells. *Eur J Immunol* 34:623-630.
43. Yadav, M., C. Louvet, D. Davini, J. M. Gardner, M. Martinez-Llordella, S. Bailey-Bucktrout, B. A. Anthony, F. M. Sverdrup, R. Head, D. J. Kuster, P. Ruminski, D. Weiss, D. Von Schack, and J. A. Bluestone. 2012. Neuropilin-1 distinguishes natural and inducible regulatory T cells among regulatory T cell subsets in vivo. *J Exp Med* 209:1713-1722, S1711-1719.
44. Weiss, J. M., A. M. Bilate, M. Gobert, Y. Ding, M. A. Curotto de Lafaille, C. N. Parkhurst, H. Xiong, J. Dolpady, A. B. Frey, M. G. Ruocco, Y. Yang, S. Floess, J. Huehn, S. Oh, M. O. Li, R. E. Niec, A. Y. Rudensky, M. L. Dustin, D. R. Littman, and J. J. Lafaille. 2012. Neuropilin 1 is expressed on thymus-derived natural regulatory T cells, but not mucosa-generated induced Foxp3+ T reg cells. *J Exp Med* 209:1723-1742, S1721.
45. Thornton, A. M., P. E. Korty, D. Q. Tran, E. A. Wohlfert, P. E. Murray, Y. Belkaid, and E. M. Shevach. Expression of Helios, an Ikaros transcription factor family member, differentiates thymic-derived from peripherally induced Foxp3+ T regulatory cells. *J Immunol* 184:3433-3441.
46. Singh, K., M. Hjort, L. Thorvaldson, and S. Sandler. Concomitant analysis of Helios and Neuropilin-1 as a marker to detect thymic derived regulatory T cells in naive mice. *Sci Rep* 5:7767.

47. Zheng, Y., A. Chaudhry, A. Kas, P. deRoos, J. M. Kim, T. T. Chu, L. Corcoran, P. Treuting, U. Klein, and A. Y. Rudensky. 2009. Regulatory T-cell suppressor program co-opts transcription factor IRF4 to control T(H)2 responses. *Nature* 458:351-356.
48. Koch, M. A., G. Tucker-Heard, N. R. Perdue, J. R. Killebrew, K. B. Urdahl, and D. J. Campbell. 2009. The transcription factor T-bet controls regulatory T cell homeostasis and function during type 1 inflammation. *Nat Immunol* 10:595-602.
49. Chaudhry, A., D. Rudra, P. Treuting, R. M. Samstein, Y. Liang, A. Kas, and A. Y. Rudensky. 2009. CD4+ regulatory T cells control TH17 responses in a Stat3-dependent manner. *Science* 326:986-991.
50. Campbell, D. J., and M. A. Koch. Phenotypical and functional specialization of FOXP3+ regulatory T cells. *Nat Rev Immunol* 11:119-130.
51. Wohlfert, E. A., J. R. Grainger, N. Bouladoux, J. E. Konkel, G. Oldenhove, C. H. Ribeiro, J. A. Hall, R. Yagi, S. Naik, R. Bhairavabhotla, W. E. Paul, R. Bosselut, G. Wei, K. Zhao, M. Oukka, J. Zhu, and Y. Belkaid. GATA3 controls Foxp3(+) regulatory T cell fate during inflammation in mice. *J Clin Invest* 121:4503-4515.
52. Pot, C., H. Jin, A. Awasthi, S. M. Liu, C. Y. Lai, R. Madan, A. H. Sharpe, C. L. Karp, S. C. Miaw, I. C. Ho, and V. K. Kuchroo. 2009. Cutting edge: IL-27 induces the transcription factor c-Maf, cytokine IL-21, and the costimulatory receptor ICOS that coordinately act together to promote differentiation of IL-10-producing Tr1 cells. *J Immunol* 183:797-801.
53. Magnani, C. F., G. Alberigo, R. Bacchetta, G. Serafini, M. Andreani, M. G. Roncarolo, and S. Gregori. 2011. Killing of myeloid APCs via HLA class I, CD2 and CD226 defines a novel mechanism of suppression by human Tr1 cells. *Eur J Immunol* 41:1652-1662.
54. Selvaraj, R. K., and T. L. Geiger. 2008. Mitigation of experimental allergic encephalomyelitis by TGF-beta induced Foxp3+ regulatory T lymphocytes through the induction of anergy and infectious tolerance. *J Immunol* 180:2830-2838.
55. Weber, S. E., J. Harbertson, E. Godebu, G. A. Mros, R. C. Padrick, B. D. Carson, S. F. Ziegler, and L. M. Bradley. 2006. Adaptive islet-specific regulatory CD4 T cells control autoimmune diabetes and mediate the disappearance of pathogenic Th1 cells in vivo. *J Immunol* 176:4730-4739.
56. Zhang, Q., F. Cui, L. Fang, J. Hong, B. Zheng, and J. Z. Zhang. TNF-alpha impairs differentiation and function of TGF-beta-induced Treg cells in autoimmune diseases through Akt and Smad3 signaling pathway. *J Mol Cell Biol* 5:85-98.
57. Brun, V., V. Neveu, Y. M. Pers, S. Fabre, B. Quatannens, H. Bastian, N. Clerget-Chossat, C. Jorgensen, and A. Foussat. 2011. Isolation of functional autologous collagen-II specific IL-10 producing Tr1 cell clones from rheumatoid arthritis blood. *Int Immunopharmacol* 11:1074-1078.
58. Floess, S., J. Freyer, C. Siewert, U. Baron, S. Olek, J. Polansky, K. Schlawe, H. D. Chang, T. Bopp, E. Schmitt, S. Klein-Hessling, E. Serfling, A. Hamann, and J. Huehn. 2007. Epigenetic control of the foxp3 locus in regulatory T cells. *PLoS Biol* 5:e38.
59. Polansky, J. K., K. Kretschmer, J. Freyer, S. Floess, A. Garbe, U. Baron, S. Olek, A. Hamann, H. von Boehmer, and J. Huehn. 2008. DNA methylation controls Foxp3 gene expression. *Eur J Immunol* 38:1654-1663.
60. Nadkarni, S., C. Mauri, and M. R. Ehrenstein. 2007. Anti-TNF-alpha therapy induces a distinct regulatory T cell population in patients with rheumatoid arthritis via TGF-beta. *J Exp Med* 204:33-39.

61. Stephens, G. L., J. Andersson, and E. M. Shevach. 2007. Distinct subsets of FoxP3+ regulatory T cells participate in the control of immune responses. *J Immunol* 178:6901-6911.
62. Apetoh, L., F. J. Quintana, C. Pot, N. Joller, S. Xiao, D. Kumar, E. J. Burns, D. H. Sherr, H. L. Weiner, and V. K. Kuchroo. The aryl hydrocarbon receptor interacts with c-Maf to promote the differentiation of type 1 regulatory T cells induced by IL-27. *Nat Immunol* 11:854-861.
63. Hegazy, A. N., M. Peine, C. Helmstetter, I. Panse, A. Frohlich, A. Bergthaler, L. Flatz, D. D. Pinschewer, A. Radbruch, and M. Lohning. Interferons direct Th2 cell reprogramming to generate a stable GATA-3(+)T-bet(+) cell subset with combined Th2 and Th1 cell functions. *Immunity* 32:116-128.
64. Amodio, G., M. Comi, D. Tomasoni, M. E. Gianolini, R. Rizzo, J. LeMaoult, M. G. Roncarolo, and S. Gregori. 2015. HLA-G expression levels influence the tolerogenic activity of human DC-10. *Haematologica*.
65. Suffia, I., S. K. Reckling, G. Salay, and Y. Belkaid. 2005. A role for CD103 in the retention of CD4+CD25+ Treg and control of Leishmania major infection. *J Immunol* 174:5444-5455.
66. Cepek, K. L., S. K. Shaw, C. M. Parker, G. J. Russell, J. S. Morrow, D. L. Rimm, and M. B. Brenner. 1994. Adhesion between epithelial cells and T lymphocytes mediated by E-cadherin and the alpha E beta 7 integrin. *Nature* 372:190-193.
67. Hanazawa, A., K. Hayashizaki, K. Shinoda, H. Yagita, K. Okumura, M. Lohning, T. Hara, S. Tani-ichi, K. Ikuta, B. Eckes, A. Radbruch, K. Tokoyoda, and T. Nakayama. CD49b-dependent establishment of T helper cell memory. *Immunol Cell Biol* 91:524-531.

802 **Figure and figure Legends**

803

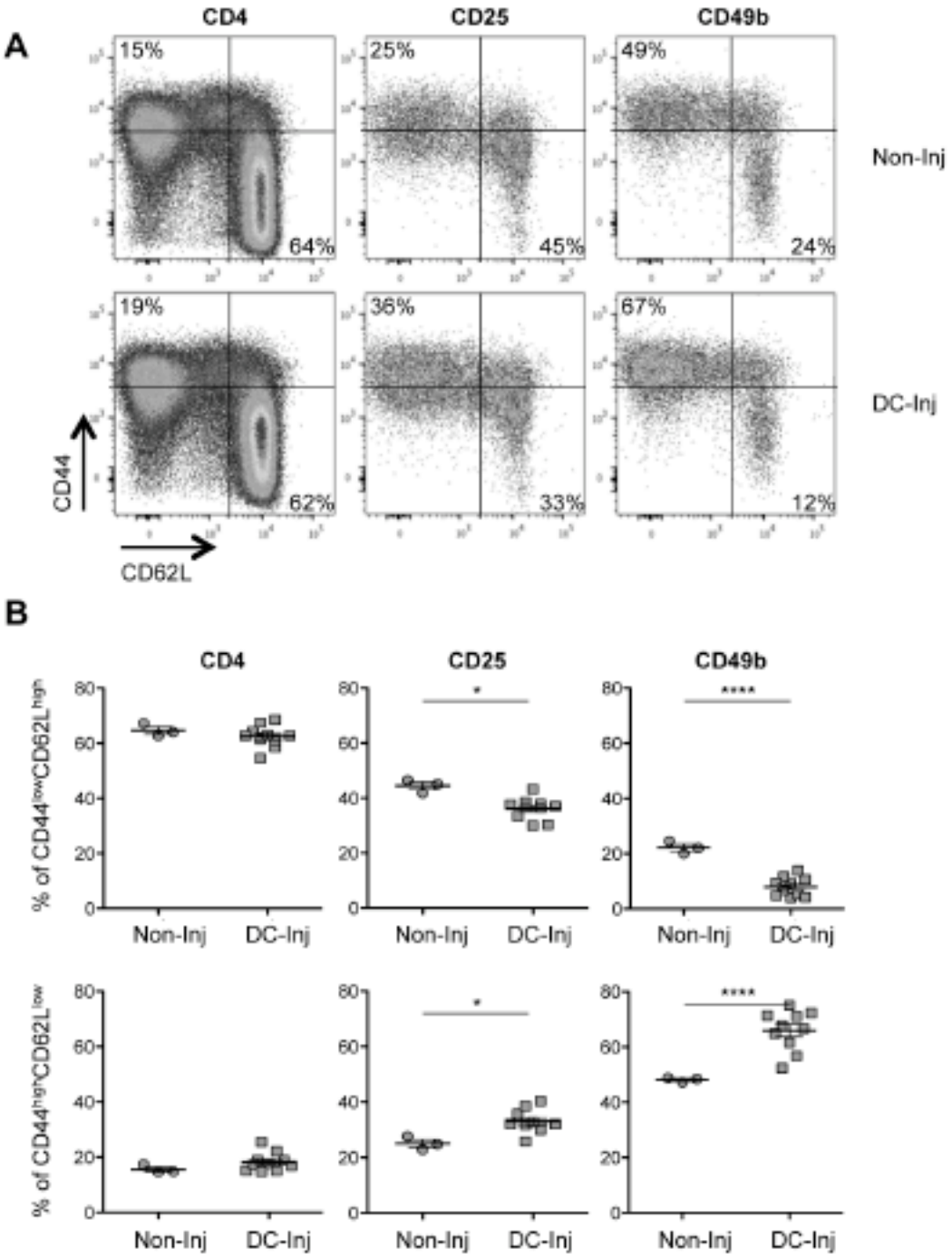

804

805 **FIGURE 1.** DC-induced CD49b^{+} cells display an effector memory phenotype.
806 Percentage of naïve (CD44^{low}CD62L^{high}) and effector memory (CD44^{high}CD62L^{low}) T
807 cells within the CD4, CD25 and CD49b gated populations (For gating strategy see

Fig S1A) were analyzed by flow cytometry for DC-injected (DC-Inj, n=10) and non-injected mice (Non-Inj, n=3). A, Representative dot plots within gated CD4 (left), CD25 (middle) and CD49b (right) positive cells in non-injected (top panels) and DC-injected mice (bottom panels). B, Percentages of naïve and effector memory cells within the gated CD4 (left), CD25 (middle) and CD49b (right) cell population. Each symbol represents an individual mouse and bars show the mean ± SEM. Data are representative of two independent experiments. * $p<0.05$, **** $p<0.0001$ by repeated measures two-way ANOVA (Bonferroni's multiple comparisons test).

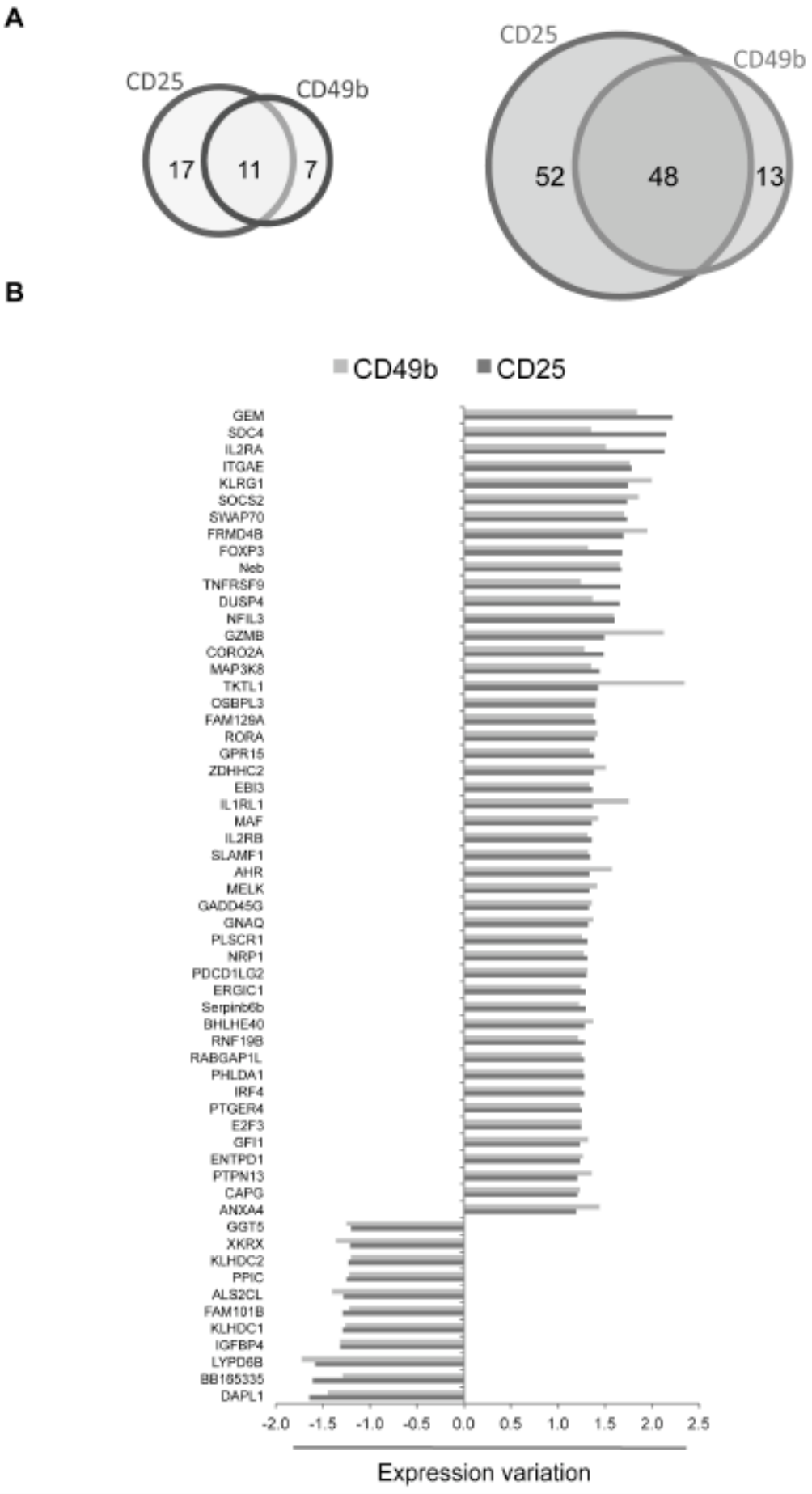
A
CD25
CD49b
17
11
7
CD25
CD49b
52
48
13
B
CD49b
CD25
GEM
SDC4
IL2RA
ITGAE
KLRG1
SOCS2
SWAP70
FRMD4B
FOXP3
Neb
TNFRSF9
DUSP4
NFIL3
GZMB
CORO2A
MAP3K8
TKTL1
OSBPL3
FAM129A
RORA
GPR15
ZDHHC2
EBI3
IL1RL1
MAF
IL2RB
SLAMF1
AHR
MELK
GADD45G
GNAQ
PLSCR1
NRP1
PDCD1LG2
ERGIC1
Serpinb6b
BHLHE40
RNF19B
RABGAP1L
PHLDA1
IRF4
PTGER4
E2F3
GFI1
ENTPD1
PTPN13
CAPG
ANXA4
GGT5
XKRX
KLHDC2
PPIC
ALS2CL
FAM101B
KLHDC1
IGFBP4
LYPD6B
BB165335
DAPL1
-2.0
-1.5
-1.0
-0.5
0.0
0.5
1.0
1.5
2.0
2.5
Expression variation

817

FIGURE 2. Transcriptional profile of CD49b$^+$ Treg cells contains multiple transcripts of the canonical Treg signature. A, Venn diagram depicting the number of commonly and uniquely down-regulated (left) or up-regulated (right) transcripts, in the FACS-sorted CD49b$^+$ and CD25$^+$ Treg cell populations, with the canonical Treg signature. B, Bar graphs show the transcriptional expression variation of the differentially expressed genes common among the CD49b$^+$, CD25$^+$ and the canonical Treg signature.

Figure 3

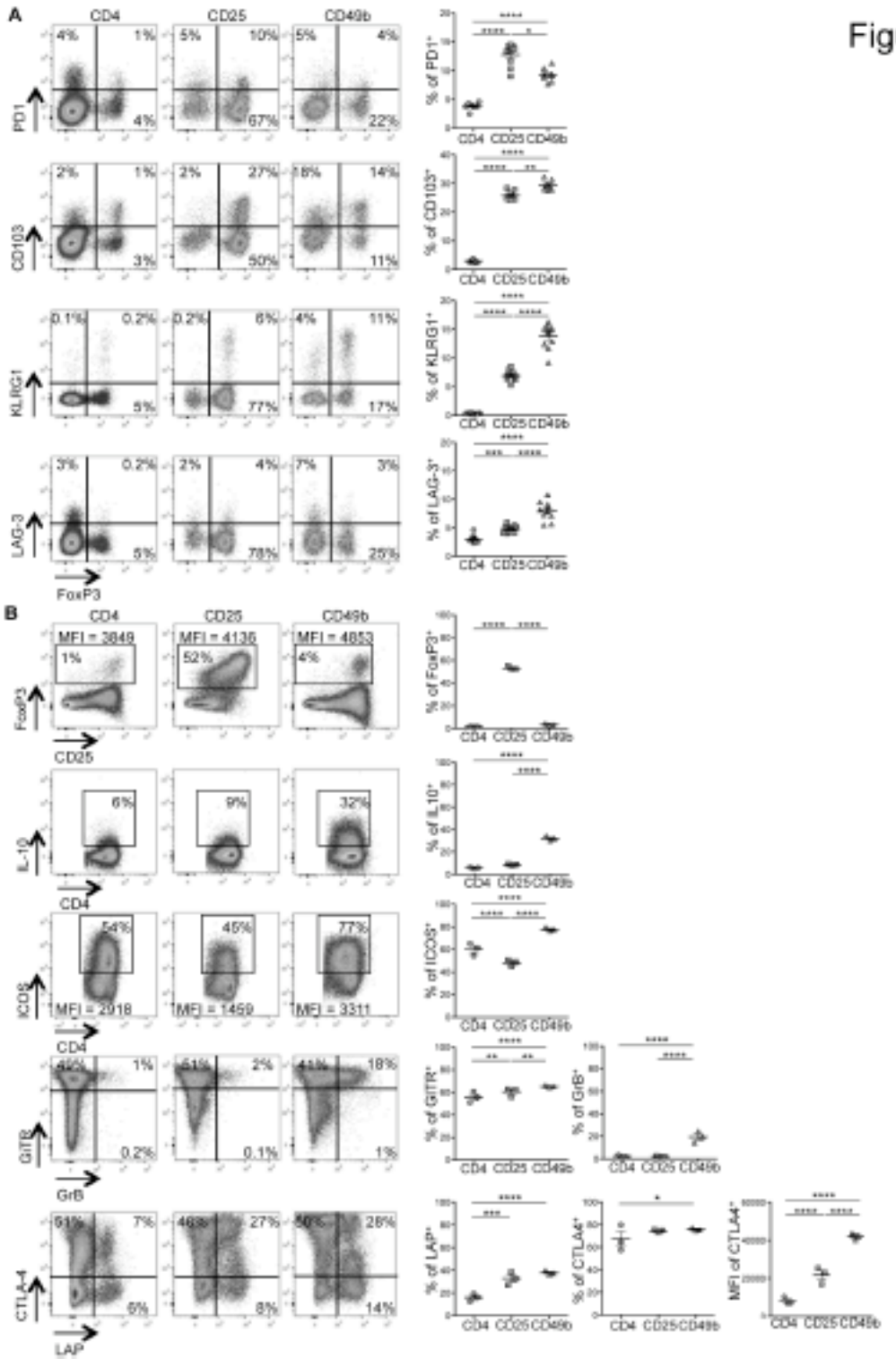

826
827 **FIGURE 3**. Several canonical markers of CD25^{+}FoxP3^{+} Treg cells are expressed by
828 CD49b^{+} effector memory cells. A, Representative flow cytometry analyses of
829 splenocytes from DC-injected mice (n=18) within the gated CD4 (left), CD25 (middle)
830 and CD49b (right) cell populations. Quadrants were set as indicated and frequencies

of cells are shown within each quadrant. Each symbol represents a pool of 2 mice and bars show the mean ± SEM. **** p<0.0001, *** p=0.0005, ** p=0.01 and * p=0.013 by repeated measures two-way ANOVA (Tukey's multiple comparisons test). B, The FACS-sorted CD4, CD25 and CD49b T cell populations from DC-vaccinated mice (n=18) were analyzed by FACS 48 hours following *in vitro* stimulation. Gates and quadrants were set as indicated and frequencies of cells are shown. Each symbol represents a pool of 6 mice and bars show the mean ± SEM. **** p<0.0001, *** p=0.0001, ** p=0.002 and * p=0.03 by repeated measures two-way ANOVA (Tukey's multiple comparisons test).

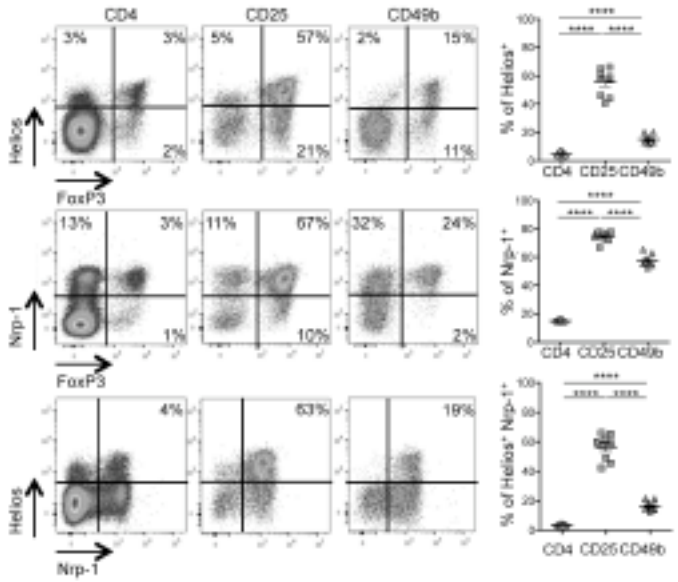

FIGURE 4. Peripherally induced CD49b^{+} cells express Neuropilin-1 without co-expressing Helios. Representative flow cytometry analyses of splenocytes from DC-injected mice (n=18) within the gated CD4 (left), CD25 (middle) and CD49b (right) cell population. Quadrants were set as indicated and percentages of Helios, Nrp-1 or double positive cells were analyzed. Each symbol represents a pool of 2 mice and bars show the mean ± SEM. **** p<0.0001 by repeated measures two-way ANOVA (Tukey's multiple comparisons test).

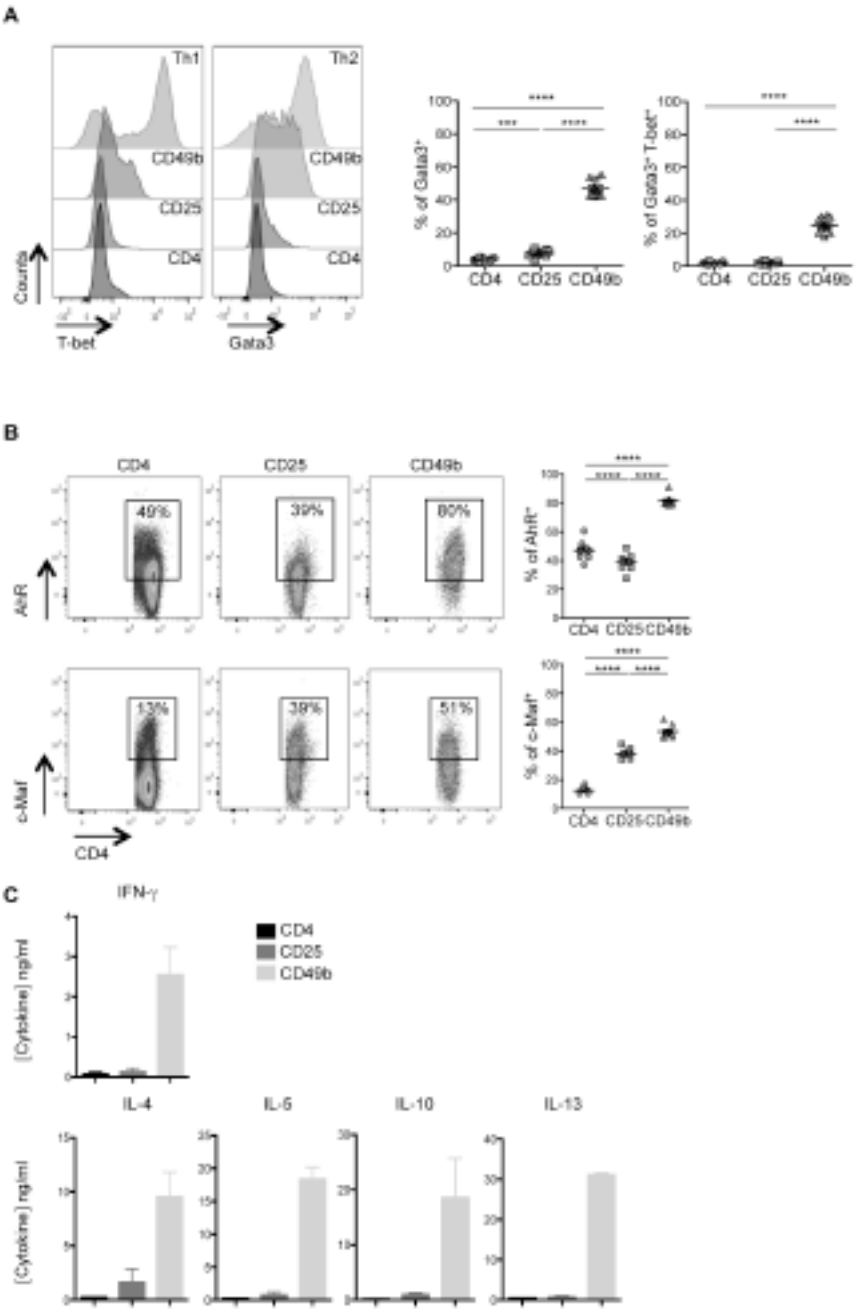

849

850 **FIGURE 5.** Peripherally induced CD49b^{+} cells express Th2-specific transcriptional
851 factors and display a dominant Th2 cytokine profile. Percentages of cells expressing
852 T-bet, Gata3 and transcriptional factors associated with IL-10 production, including c-
853 Maf and AhR, were analyzed within the gated CD4, CD25 and CD49b cell
854 populations from DC-injected splenocytes (n=18). A, Representative histogram plots
855 of T-bet and Gata3 staining in gated CD4, CD25 and CD49b cell populations were

compared to *in vitro* polarized Th1 and Th2 cells. Percentages of Gata3$^+$ and double positive Gata3$^+$T-bet$^+$ cells are represented with mean ± SEM, each symbol representing a pool of 2 mice. Data are representative of two independent experiments. **** p<0.0001, *** p=0.0003 by repeated measures two-way ANOVA (Tukey's multiple comparisons test). B, Representative dot plots and percentages of AhR$^+$ and c-Maf$^+$ cells in gated CD4, CD25 and CD49b cell populations. Each symbol represents a pool of 2 mice and bars show the mean ± SEM. Data are representative of two independent experiments. **** p<0.0001 by repeated measures one-way ANOVA (Tukey's multiple comparisons test). C, Level of cytokine secretion by highly purified cells following *in vitro* activation.

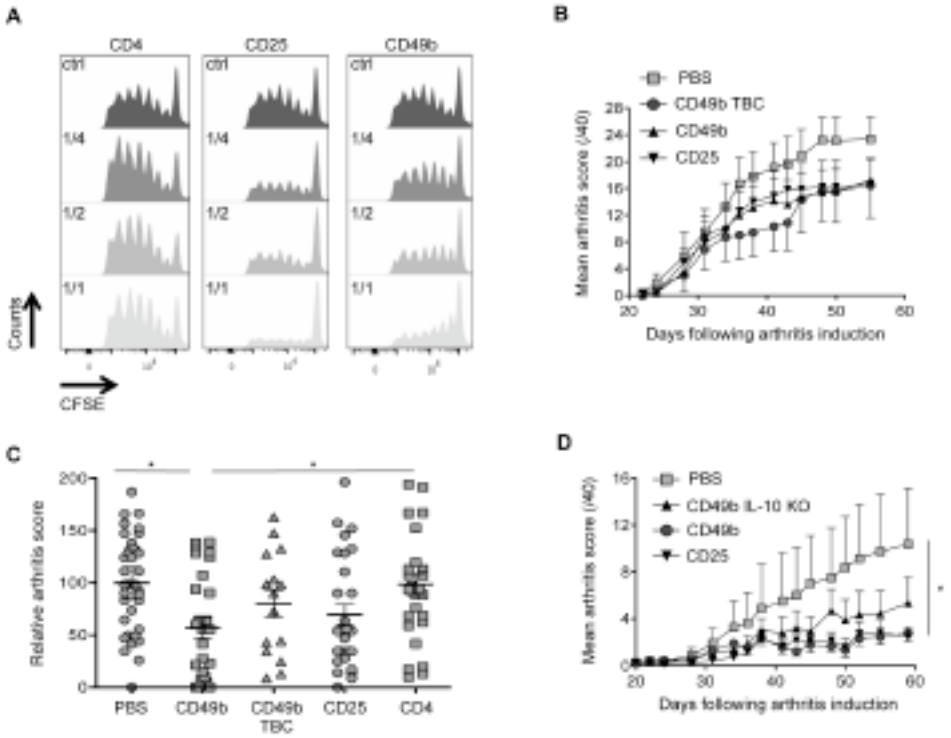

FIGURE 6. Polyclonal and Ag-specific CD49b$^+$ T reg cells display potent *in vitro* and *in vivo* suppressive capacities. A, Comparable suppressive capacities of FACS-sorted CD25$^+$ and CD49b$^+$ Treg cells *in vitro***.** CFSE-labeled effector T (Teff) cells

were cultured in activating conditions with titrated numbers of $CD4^+$, $CD25^+$ or $CD49b^+$ T cell population at different Treg/Teff ratios. As positive control for T cell proliferation, Teff cells were cultured alone in activating conditions (ctrl). Results are representative of three independent experiments. B, C, D, Comparison of the suppressive function of Treg cells *in vivo* in the experimental model of CIA. Mice were intravenously injected with 150,000 FACS-sorted T cells or with PBS on day 28 after immunization. Means of the severity scores of arthritis are represented for each group with a maximal score of 40 per mouse. B, Comparison of the therapeutic potential of polyclonal $CD49b^+$ (CD49b) and $CD25^+$ (CD25) Treg cells isolated from syngeneic DBA/1 mice as well as Ag-specific $CD49b^+$ cells (CD49b TBC) isolated from TBC mice. Data are represented as mean ± SEM of each group. C, Relative arthritic scores were calculated for each independent experiment using the mean of the PBS-treated mice (PBS, 5 independent experiments) as 100% disease severity. Each symbol represents a mouse and bars represent the mean ± SEM. Results obtained with polyclonal $CD49b^+$ (CD49b, 4 independent experiments), Ag-specific $CD49b^+$ (CD49bTBC, 2 independent experiments), and $CD25^+$ (CD25, 4 independent experiments) Treg cells as well as $CD4^+$ T cells treated mice (CD4, 4 independent experiments) are represented. * $p<0.05$ by one-way ANOVA (Tukey's multiple comparisons test). D, The suppressive mechanism of $CD49b^+$ Treg cells is partially dependent on IL-10. Therapeutic potential of $CD49b^+$ Treg cells FACS-sorted from IL-10 KO mice (CD49b IL-10 KO) or from wild-type littermates (CD49b), and $CD25^+$ Treg cells FACS-sorted from wild-type littermates (CD25) were compared in CIA (n=7 to 9 mice per group). Data are represented as mean ± SEM of each group, and are representative of 2 independent experiments. * $p<0.05$ by repeated measures two-way ANOVA (Tukey's multiple comparisons test). Significant differences were

observed from days 50 to 59 for CD49b treated mice compared with PBS-injected mice; and from day 59 for CD25 treated mice compared with PBS-injected mice.